



Synthesis, characterization, biological screenings and interaction with calf thymus DNA of a novel azomethine 3-((3,5-dimethylphenylimino)methyl)benzene-1,2-diol

Muhammad Sirajuddin^a, Saqib Ali^{a,*}, Naseer Ali Shah^b, Muhammad Rashid Khan^b,
Muhammad Nawaz Tahir^c

^a Department of Chemistry, Quaid-i-Azam University, Islamabad 45320, Pakistan

^b Department of Biochemistry, Quaid-i-Azam University, Islamabad 45320, Pakistan

^c Department of Physics, University of Sargodha, Pakistan

ARTICLE INFO

Article history:

Received 1 February 2012

Received in revised form 13 March 2012

Accepted 21 March 2012

Keywords:

Schiff base

Crystal structure

CTDNA interaction

Antibacterial activity

Antifungal activity

Cytotoxicity

DPPH

ABSTRACT

The novel azomethine, 3-((3,5-dimethylphenylimino)methyl)benzene-1,2-diol (HL) was synthesized and characterized by elemental analysis, FT-IR, ¹H, ¹³C NMR spectroscopy and single crystal analysis. The title compound has been screened for its biological activities including enzymatic study, antibacterial, antifungal, cytotoxicity, antioxidant and interaction with CTDNA, and showed remarkable activities in each area of research. The titled compound interacts with DNA via two binding modes: intercalation and groove binding. In intercalation the compound inserts itself into the base pairs of DNA and the compound–DNA complex is stabilized by π – π stacking. Interaction via groove binding may be due to hydrogen bonding to bases, typically to N3 of adenine and O2 of thymine. The synthesized compound was also found to be an effective antioxidant of 2,2-diphenyl-1-picrylhydrazyl radical (DPPH) and gives percent inhibition (%) of 90.7 at a concentration level of 31.3 μ g/mL.

© 2012 Elsevier B.V. All rights reserved.

1. Introduction

Azomethines (Schiff bases) have been widely studied as they possess many interesting features, including photochromic and thermochromic properties, proton transfer tautomeric equilibria, biological and pharmacological activities, as well as suitability for analytical applications [1]. They show biological applications including antibacterial [2–7], antifungal [4–7] and antitumor activity [8]. Diamino tetradentate azomethines, e.g., N,N-bis(1-naphthaldimine)-o-phenylenediamine, and their metal complexes, e.g., lanthanide metal complexes [LnL(NO₃)₂(H₂O)_x](NO₃)₃ {Ln(III)=Nd, Dy, Sm, Pr, Gd, Tb, La and Er, L=N,N-bis(1-naphthaldimine)-o-phenylenediamine, X=0 for Nd, Sm, 1 for La, Gd, Pr, Nd, Dy, and 2 for Tb} [9] have been used as biological models to understand the structures of biomolecules and biological processes. For example transition metals occur in metalloenzyme bound to a macrocycle such as a heme ring or to donor atoms of peptide chains usually in a distorted environment, as in hemerythrin (Fe₂) or hemocyanin (Cu₂). Symmetric tetradentate Schiff

base (TSB) complexes of cobalt(II) have been used extensively as macrocycle models, while asymmetric complexes are required to model the irregular binding of peptides [10]. The Schiff bases are found to act as tetradentate ligands using N₂O₂ donor set of atoms leading to a square-planar geometry for the complexes around all the metal ions [11]. The use of Schiff base as neutral carriers have been reported as ion selective electrodes for determination of metal cations such as copper(II), mercury(II), nickel(II), silver(II), lead(II), cobalt(III) gadolinium(III), yttrium(III), dysprosium(III) [12]. Azomethines ligands are considered as “privileged ligands” due to their ease of preparation and their use as fluorogenic agent, pesticides, herbicidal agents, blocking agents, as well as in catalysis [13,14].

Design and synthesis of novel and potent DNA-targeted compounds have important theoretical significance and application value in chemistry, biology and medicine fields. Such compounds include DNA-alkylating agents, DNA groove binders and DNA intercalators. DNA-intercalating molecules are those which intercalate DNA base pairs via electron-deficient planar chromophores with flexible side chains. These specially designed groups confer DNA sequence selectivity and allow aromatic heterocycles to position at proper sites or interact with topoisomerases so as to interfere with DNA replication and transcription [15,16]. Acridine,

* Corresponding author. Tel.: +92 51 90642130; fax: +92 51 90642241.
E-mail address: drsa54@yahoo.com (S. Ali).

naphthodiazine and anthraquinone are all famous intercalating matrixes [17]. DNA binding is the critical step for DNA activity [10].

In the recent study we synthesized 3-((3,5-dimethylphenylimino)methyl)benzene-1,2-diol successfully and characterized it by various techniques. Biological activities including DNA interaction, enzymatic study, antibacterial, anti-fungal, cytotoxic and antioxidant activities of the titled compound were studied. We have found that the titled compound show remarkable activities in each area of research.

2. Experimental

2.1. Materials

Reagents, 3,5-dimethylaniline and 2,3-dihydroxybenzaldehyde were obtained from Aldrich (USA) and were used without further purification. Sodium salt of CTDNA (Arcos) was used as received. All the solvents purchased from E. Merck (Germany) were dried before use according to the literature procedure [18].

2.2. Physical measurements

The melting point was determined in a capillary tube using a Gallenkamp (U.K.) electrothermal melting point apparatus. IR spectrum in the range of 4000–400 cm^{-1} was obtained on a Thermo Nicolet-6700 FT-IR Spectrophotometer. Microanalysis was done using a Leco CHNS 932 apparatus. ^1H and ^{13}C NMR were recorded on a Bruker-300 MHz FT-NMR Spectrometer, using CDCl_3 as an internal reference [^1H (CDCl_3) = 7.25 and ^{13}C (CDCl_3) = 77]. Chemical shifts are given in ppm and coupling constants (J) values are given in Hz. The multiplicities of signals in ^1H NMR are given with chemical shifts (s = singlet, d = doublet, t = triplet, m = multiplet). The absorption spectrum was measured on a Shimadzu 1800 UV-Visible Spectrophotometer. The electrical conductance was measured on a WTW Series Inolab Cond 720. The GC-MS spectrum was taken on a gas chromatograph, model GC-6890N coupled with mass spectrometer, model MS-5973 MSD (mass selective detector). Separation was performed on a capillary column DB-5MS (30 m \times 0.32 mm, 0.25 μm of film thickness). The mass Spectrometer coupled with GC was set to scan in the range of m/z 50–550 with electron impact (EI) mode of ionization. The X-ray diffraction data were collected on a Bruker SMART APEX CCD diffractometer, equipped with a 4 K CCD detector set 60.0 mm from the crystal. The crystals were cooled to 100 ± 1 K using the Bruker KRYOFLEX low temperature device and intensity measurements were performed using graphite monochromated Mo-K α radiation from a sealed ceramic diffraction tube (SIEMENS). Generator settings were 50 kV/40 mA. The structure was solved by Patterson methods and extension of the model was accomplished by direct methods using the program DIRDIF or SIR2004. Final refinement on F^2 carried out by full-matrix least squares techniques using SHELXL-97, a modified version of the program PLUTO (preparation of illustrations) and PLATON package.

2.2.1. DNA interaction study by UV-Visible spectroscopy

CTDNA (20 mg) was dissolved and stirred for overnight in double deionized water (pH = 7.0) and kept at 4 $^\circ\text{C}$ for less than 4 days. The nucleotide to protein (N/P) ratio of ~ 1.9 was obtained from the ratio of absorbance at 260 and 280 nm ($A_{260}/A_{280} = 1.9$), indicating that

the DNA is sufficiently free from protein [19]. The DNA concentration was determined via absorption spectroscopy using the molar absorption coefficient of $6600 \text{ M}^{-1} \text{ cm}^{-1}$ (260 nm) for CTDNA [20] and was found to be $2.37 \times 10^{-5} \text{ M}$. The compound was dissolved in 80% ethanol at a concentration of 0.392 mM. The UV absorption titrations were performed by keeping the concentration of the compound fixed while varying the CTDNA concentration. Equivalent solutions of CTDNA were added to the complex and reference solutions to eliminate the absorbance of DNA itself. Compound-CTDNA solutions were allowed to incubate for 30 min at room temperature before measurements were made. Absorption spectra were recorded using cuvettes of 1 cm path length at room temperature (25 ± 1 $^\circ\text{C}$).

2.2.2. Viscosity measurements

Viscosity measurements were carried out using Ubbelohde viscometer at room temperature (25 ± 1 $^\circ\text{C}$). Flow time was measured with a digital stopwatch. Each sample was measured three times and an average flow time was calculated. Data were presented as relative viscosity, $(\eta/\eta_0)^{1/3}$, vs. binding ratio ($[\text{HL}]/[\text{DNA}]$) where η is the viscosity of DNA in the presence of complex and η_0 is the viscosity of DNA alone. Viscosity values were calculated from the observed flow time of DNA containing solution (t_0), $\eta = t - t_0$ [21].

2.2.3. Cyclic voltammetry

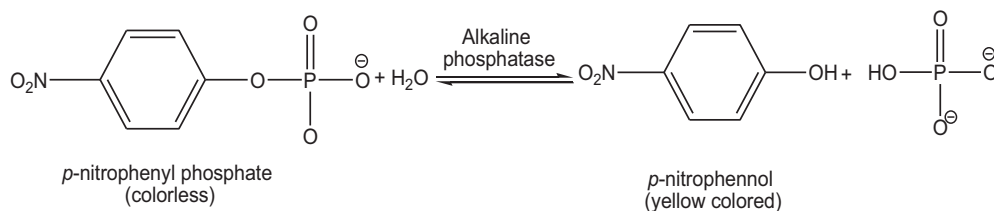
Voltammetric experiments were carried out using a $\mu\text{Autolab}$ running with GPES 4.9 software, Eco-Chemie, Utrecht, the Netherlands. Measurements were carried out using a glassy carbon working electrode (GCE) with a geometric area of 0.071 cm^2 , a Pt wire counter electrode and a saturated calomel reference electrode (SCE), in one-compartment electrochemical cell. The GCE was cleaned by polishing with $1 \mu\text{m}$ alumina paste and rinsed with water before each experiment. Stock solution 3 mM of HL was prepared in 10% aqueous DMSO at pH = 7.0 (phosphate buffer). All experiments were done at room temperature (25 ± 1 $^\circ\text{C}$).

2.2.4. Enzymatic activity

2.2.4.1. Assay of alkaline phosphatase inhibition. The inhibition of alkaline phosphatase was assayed by monitoring the rate of hydrolysis of *p*-nitrophenyl phosphate at 25 $^\circ\text{C}$ in 0.1 M Na_2CO_3 – NaHCO_3 (sodium carbonate–bicarbonate) buffer (pH = 10.1) [22,23]. The enzyme catalyzes the hydrolysis of phosphate monoesters resulting in the formation of inorganic phosphate and an alcohol. The identity of the alcohol varies depending on the specific phosphatase. The assay of alkaline phosphatase activity takes advantage of the fact that the enzyme is non-specific and utilizes the non-biological substrate *p*-nitrophenyl phosphate (colorless) to give yellow colored *p*-nitrophenol upon hydrolysis which helps to monitor the reaction as shown in Scheme 1 [23].

Stock solution of 50 μM inhibitor (HL) in 1 mL DMSO was prepared at room temperature. The buffer and substrate were mixed in 1:4 ratios to make the reagent solution. Then from the reagent solution 2000 μL (2 mL) was taken in the cell and to which 40 μL enzyme and varying concentrations of the inhibitor were added. The spectrum of the alkaline phosphatase in the presence and absence of inhibitor was measured using UV-Visible Spectrophotometer. The release of yellow colored *p*-nitrophenol chromophore was monitored at 405 nm wavelength. Enzyme activity has been expressed as the μM of *p*-nitrophenol released per min for 5 min for each concentration of the inhibitor and then take their average value. The inhibition of enzyme by inhibitor was calculated by the following formula [24]:

$$\text{Units/mL enzyme} = \frac{(\Delta A_{405 \text{ nm}} / \text{min Test} - \Delta A_{405 \text{ nm}} / \text{min Blank}) \text{ total VmL}(\text{reagent} + \text{enzyme} + \text{inhibitor}) \times \text{D.F.}}{18.5 \times \text{VmL of enzyme taken}}$$



Scheme 1.

D.F. = dilution factor; 18.5 = millimolar extinction coefficient of *p*-nitrophenol at 405 nm.

By the addition of increasing amounts of inhibitor the activity of the enzyme decreased and at higher concentration it was almost completely inhibited as shown in Fig. 7.

2.2.5. Antibacterial assay

The synthesized compound was tested against six bacterial strains: two Gram-positive [*Micrococcus luteus* (ATCC10240) and *Staphylococcus aureus* (ATCC6538)] and four Gram-negative [*Escherichia coli* (ATCC15224), *Pseudomonas aeruginosa* (CM0559),

Bordetella bronchiseptica (ATCC4617) and *Klebsiella pneumoniae* (MTCC618)]. The agar well-diffusion method was used for the determination of antibacterial activity [25]. Broth culture (0.75 mL) containing ca. 10^6 colony forming units (CFU) per mL of the test strain was added to 75 mL of nutrient agar medium at 45 °C, mixed well, and then poured into a 14 cm sterile petri plate. The media was allowed to solidify, and 8 mm wells were dug with a sterile metallic borer. Then a DMSO solution of test sample (100 µL) at 1 mg/mL was added to the respective wells. DMSO served as negative control, and the standard antibacterial drugs *Roxithromycin* (1 mg/mL) and *Cefixime* (1 mg/mL) were used as positive control. Triplicate plates of each bacterial strain were prepared which were incubated aerobically at 37 °C for 24 h. The activity was determined by measuring the diameter of zone showing complete inhibition (mm).

2.2.6. Antifungal assay

Antifungal activity against five fungal strains [*Fusarium moniliformis*, *Aspergillus niger*, *Fusarium solani*, *Mucor* species and *Aspergillus fumigatus*] was determined by using agar tube dilution method [25]. Screw capped test tubes containing sabouraud dextrose agar (SDA) medium (4 mL) were autoclaved at 121 °C for 15 min. Tubes were allowed to cool at 50 °C and non solidified SDA was loaded with 66.6 µL of compound from the stock solution (12 mg/mL in DMSO) to make 200 µg/mL final concentration. Tubes were then allowed to solidify in slanting position at room temperature. Each tube was inoculated with 4 mm diameter piece of inoculum from seven days old fungal culture. The media supplemented with DMSO and *Turbinafine* (200 µL/mL) were used as negative and positive control, respectively. The tubes were incubated at 28 °C for 7 days and growth was determined by measuring linear growth (mm) and growth inhibition was calculated with reference to the negative control.

2.2.7. Cytotoxicity

Cytotoxicity was studied by the brine-shrimp lethality assay method [25,26]. Brine-shrimp (*Artemia salina*) eggs were hatched in artificial sea water (3.8 g sea salt/L) at room temperature (22–29 °C). After two days these shrimps were transferred to vials containing 5 mL of artificial sea water (10 shrimps per vial) with 10, 100 and 1000 µg/mL final concentrations of each compound taken from their stock solutions of 12 mg/mL in DMSO. After 24 h number of surviving shrimps was counted. Data were analyzed with a biostat 2009 computer programme (Probit analysis) to determine LD₅₀ values.

2.2.8. Scavenging effect on 2,2-diphenyl-1-picrylhydrazyl (DPPH)

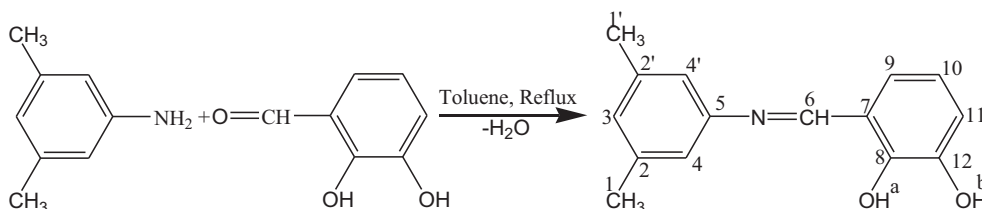
The solution of 2,2-diphenyl-1-picrylhydrazyl (DPPH) radical was obtained by dissolving 3.94 mg of DPPH in 100 mL methanol. To 2.8 mL of the methanolic solutions of DPPH, 0.2 mL of HL solution with different concentration ranging from 0.0625 mg/mL to 1.0 mg/mL was added [27–29]. After 10 min the decrease in absorption was measured at 517 nm of DPPH using UV–Visible Spectrophotometer. The actual decrease in absorption was measured against that of the control and the percentage inhibition was calculated. The same experiment was carried out on ascorbic acid which is known antioxidant. All test and analysis were run in triplicates and the results obtained were averaged.

2.3. Synthesis

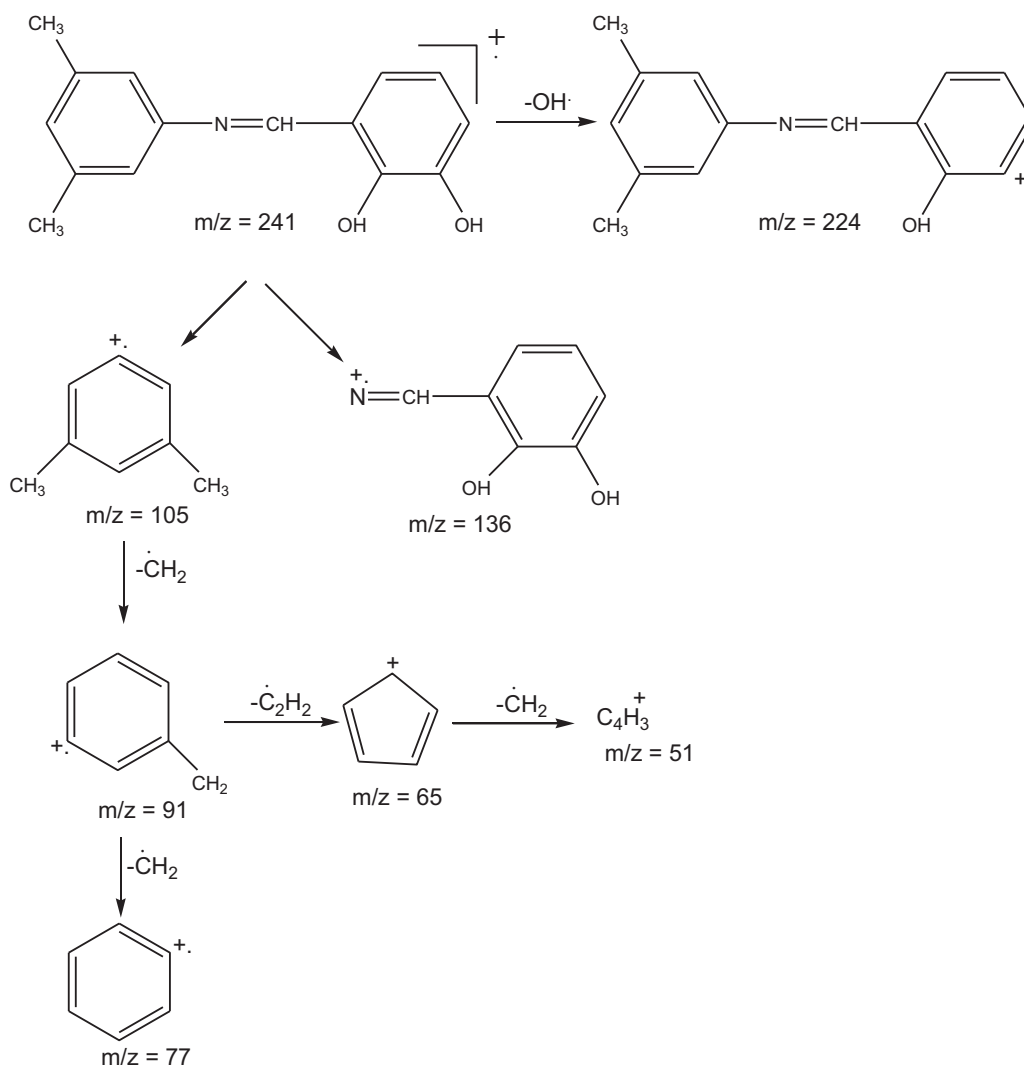
3-((3,5-dimethylphenylimino)methyl)benzene-1,2-diol (HL)

Stoichiometric amounts of 3,5-dimethylamine and 2,3-dihydroxybenzaldehyde (5 mmol of each) were added to freshly dried toluene. The mixture was refluxed for 3–4 h and the water formed was removed by using Dean and Stark apparatus. The reaction mixture volume was reduced to one-third of its original and left for crystallization at room temperature. The dark red crystals of HL suitable for a single crystal analysis were isolated from the mother liquor and dried. The chemical reaction is shown in Scheme 2.

Yield: 85%, m.p.: 134–135 °C, Mol. Wt.: 241, Anal. Calc. for C₁₅H₁₅NO₂: C, 74.67; H, 6.27; N, 5.81; Found: C, 74.60; H, 6.30; N, 5.80%, IR (cm⁻¹): ν 1604 (C=N), 1405 and 1589 (Ar C=C), 3421 (free OH), 3341 (H-bonded OH), 1205–1357 (Phen. C–O Str. vib.), ¹H NMR (CDCl₃, ppm): 2.39 (s, 6H, H1, H1'), 6.98 (s, 1H, H3), 6.95 (s, 2H, H4, H4'), 8.60 (s, 1H, H6), 7.03–7.07 (dd, 1H, H9), 6.8–6.85 (t, 1H, H10, ³J[¹H–¹H] = 7.8), 6.97–6.98 (d, H11), 5.85 (s, OH^a), 14.08



Scheme 2.



Scheme 3.

(s, OH^b, N...H–O); ¹³C NMR (CDCl₃, ppm): 21.3 (2C, C1, C1'), 139.3 (2C, C2, C2'), 128.9 (1C, C3), 118.7 (2C, C4, C4'), 159.1 (1C, C5), 161.4 (1C, C6), 118.1 (1C, C7), 152.1 (1C, C8), 123.3 (1C, C9), 122.8 (1C, C10), 119 (1C, C11), 146.9 (1C, C12); Molar conductance in 80% ethanol (Λ_m , S cm² mol⁻¹): 16 at 25 °C, Solubility: chloroform, toluene, ethanol, methanol and DMSO.

3. Results and discussion

The azomethine is prepared as described in the experimental part, crystallized, dried and subjected to elemental analyses. The results of elemental analyses (C, H, N) obtained are in good agreement with those calculated for the suggested formula. The sharp melting point indicates the purity of the synthesized azomethine. The structure of azomethine (HL) is given in Scheme 1 which is also confirmed by IR, ¹H and ¹³C NMR spectra and single crystal analysis. The electron impact mass spectrum of HL is recorded and fragmentation pattern is given in Scheme 3.

3.1. Mass spectrometry

The possible suggested molecular ion fragments are given in Scheme 3, while its GC–MS spectrum is shown in Fig. 1. In Fig. 1 (A) represent the GC spectrum while (B) represent the MS spectrum.

The GC spectrum contains only a single peak. The compound showed a molecular ion peak (parent peak) of maximum intensity with $m/z=241$. The initial fragmentation is due to the loss of a hydroxyl group giving ion peak at $m/z=224$ which is of second maximum intensity. The molecular ion peak undergoes two major fragmentation pathways with $m/z=105$ and 136. The former undergoes cleavage to give ion peak at $m/z=91$ by the elimination of methylene group (CH₂) and then to give ion peak at $m/z=77$ which can be attributed to the phenyl radical ion. The fragment of $m/z=91$ eliminates C₂H₂ group to give ion peak at $m/z=65$ with another route which then gives ion peak at $m/z=51$ by the elimination of CH₂ group.

3.2. IR spectroscopy

In the IR spectrum of HL a sharp band observed at 3421 cm⁻¹ is assigned to free (ν O–H) while a broad band observed at 3341 cm⁻¹ is assigned to hydrogen bonded (ν O–H). A strong band attributable to (ν C=N) is observed at 1604 cm⁻¹. The stretching vibration of phenolic C–O band occurs at 1205–1357. The stretching vibration bands of aliphatic and aromatic C–H group are observed at 2914 and 3040 cm⁻¹, respectively. A CH₃ bending vibration is observed at 1389 cm⁻¹.

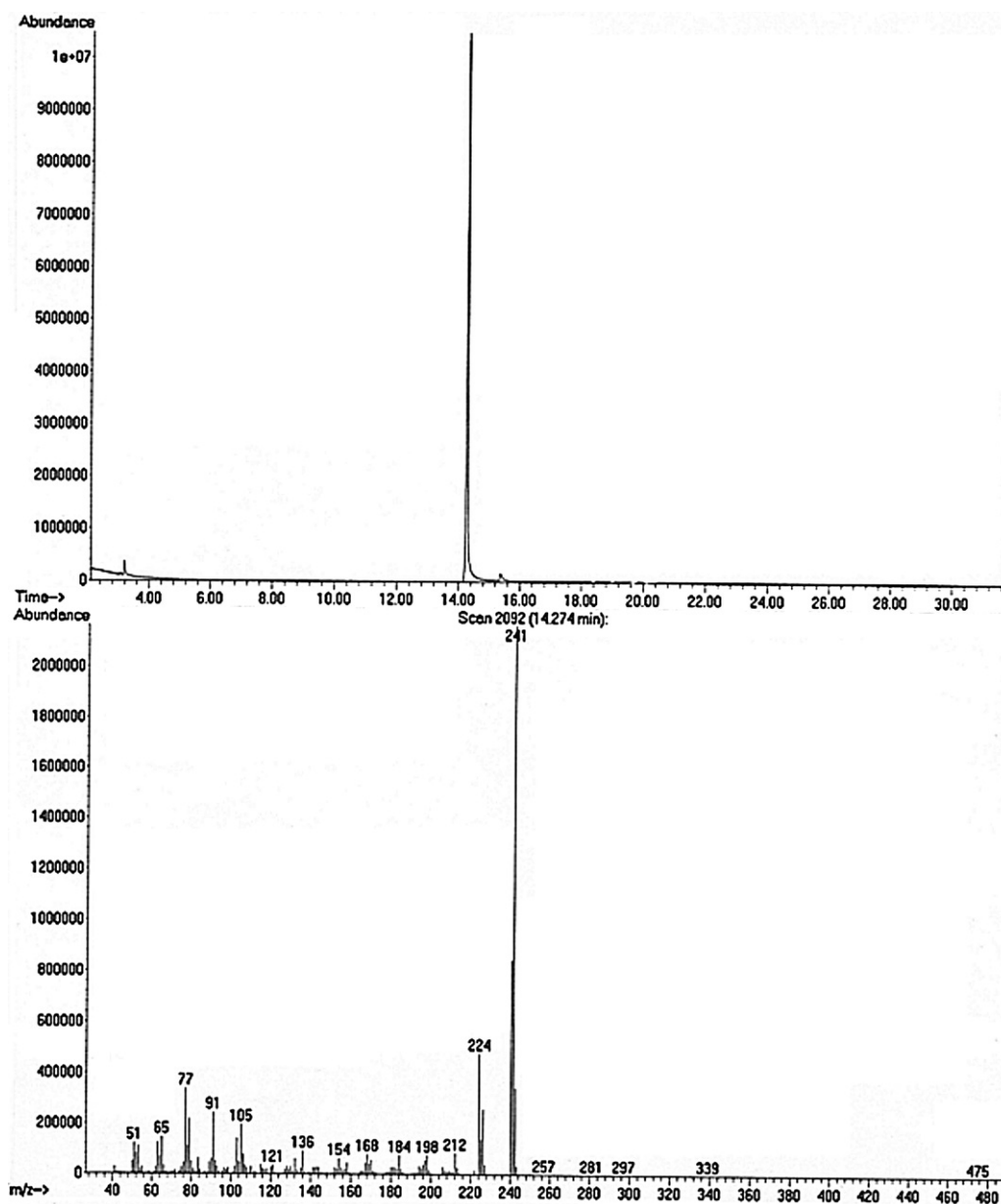


Fig. 1. Total ion chromatogram of HL.

3.3. NMR spectroscopy

The NMR spectrum of HL was recorded in chloroform (CDCl_3). The chemical shifts of the different types of protons and carbons are given in experimental part. The formation of HL was supported by the appearance of a sharp singlet at 8.60 ppm, corresponding to the azomethine proton ($-\text{N}=\text{CH}-$). One hydroxyl proton gives a singlet at 5.85 ppm (OH^a) while the other at 14.08 ppm (OH^b). This downfield shifting of OH^b is due to strong intramolecular $\text{O}-\text{H}\cdots\text{N}$ hydrogen bonding, to which the chemical shift of the proton is very sensitive. In the ^{13}C NMR spectrum the peak at 161.4, belongs to the azomethine carbon (C-6). The remaining peaks are described in the same positions as calculated by incremental methods [30].

3.4. Crystal structure of HL

The molecular structure of 3-((3,5-dimethylphenylimino)methyl)benzene-1,2-diol (HL) is shown in Fig. 2 while crystal data, selected bond distances and angles

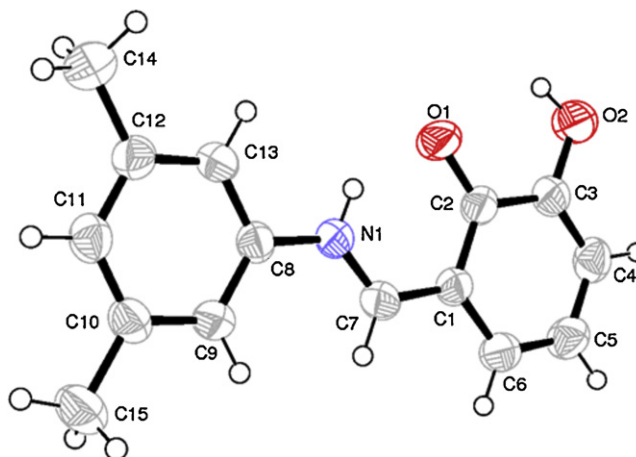


Fig. 2. ORTEP drawing of HL with atomic numbering scheme.

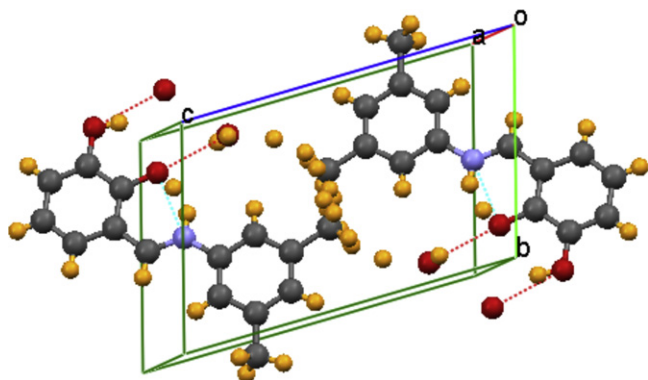
Table 1
Crystal data and structure refinement parameters for HL.

Formula	C ₁₅ H ₁₅ NO ₂
Formula weight	241.28
Crystal system	Triclinic
Space group	<i>P</i> $\bar{1}$ (No. 2)
<i>a</i> (Å)	7.5598(10)
<i>b</i> (Å)	7.6837(10)
<i>c</i> (Å)	11.4815(16)
α (°)	74.433(4)
β (°)	75.663(5)
γ (°)	85.707(5)
<i>V</i> (Å ³)	622.43(15)
<i>Z</i>	2
<i>d</i> (g cm ⁻³)	1.287
μ (Mo K α) (mm ⁻¹)	0.086
<i>F</i> (000)	256
Crystal habit/size (mm)	Needle/0.26 × 0.14 × 0.12
<i>T</i> (K)	296(2)
Radiation (Å) (Mo K α)	0.71073
θ Min–Max (°)	2.75–25.25
Total reflections	2229
Tot., Uniq. Data, <i>R</i> (int)	2229, 1670, 0.0256
Observed data [<i>I</i> > 0.0 sigma(<i>I</i>)]	1670
<i>N</i> ref, <i>N</i> par	2229, 157
$w = 1/[\sigma^2(F_o)^2 + (0.0560P)^2 + 0.1512P]$ where $P = [(F_o)^2 + 2(F_c)^2]/3$	
<i>R</i> , <i>wR</i> ₂ , <i>S</i>	0.0463, 0.1083, 1.047
Max. and Av. shift/error	0.00, 0.00
Min. and Max. Resd. Dens. [e/Å ³]	-0.198, 0.162
Goodness-of-fit	1.044

Table 2
Selected bond lengths (Å) and bond angles (°) for ligand HL.

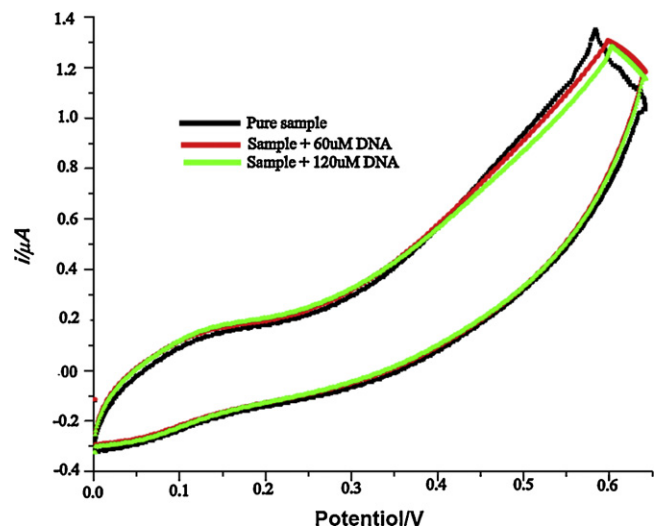
<i>Bond lengths</i>			
O1–C2	1.2986(18)	O2–C3	1.3516(19)
N1–C8	1.4132(19)	N1–C7	1.2961(19)
C1–C7	1.416(2)	C1–C2	1.415(2)
C1–C6	1.407(2)	C2–C3	1.422(2)
C3–C4	1.355(2)	C8–C9	1.381(2)
C11–C12	1.383(2)	C10–C15	1.502(2)
<i>Bond angles</i>			
C7–N1–C8	127.95(12)	C2–C1–C7	119.34(14)
C6–C1–C7	120.57(14)	C2–C1–C6	120.08(14)
O1–C2–C1	123.29(14)	O1–C2–C3	118.91(14)
C1–C2–C3	117.80(14)	O2–C3–C4	120.92(15)
C2–C3–C4	120.49(15)	O2–C3–C2	118.59(14)
C3–C4–C5	121.33(16)	N1–C7–C1	121.90(14)
N1–C8–C13	116.29(13)	C13–C12–C14	120.07(13)

are given in Tables 1 and 2, respectively. The compound exists as a monomer. The two hydroxyl groups are *cis* to each other. The hydroxyl H atom is involved in an intramolecular interaction with the imine N atom as shown in Fig. 3. Details of hydrogen bonds are given in Table 3.

**Fig. 3.** The molecular packing of HL viewed along the *b*-axis. The dotted lines show the intramolecular H-bonding.**Table 3**
Hydrogen-bond geometry (Å, °) for ligand HL.

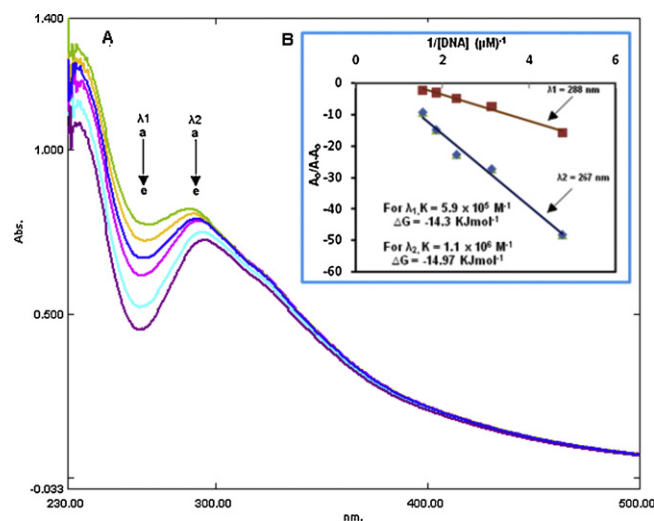
D–H...A	D–H	H...A	D...A	D–H...A
N1–H1...O1	0.8600	1.8300	2.5465(16)	140.00
O2–H2...O1	0.8500	2.2600	2.6974(15)	113.00
O2–H2...O1	0.8500	1.9800	2.7527(13)	151.00

Symmetry codes: (i) 1 – *x*, 2 – *y*, –*z*; (ii) 2 – *x*, 1 – *y*, –*z*; (iii) *x*, 1 + *y*, –1 + *z*.

**Fig. 4.** CV behavior of 3 mM sample in 10% aqueous DMSO at 100 mV/s, 0.1 M KCl as supporting electrolyte and pH 7.0 phosphate buffer.

3.5. Cyclic voltammetry

For exploring the binding mode between the HL and CTDNA, the CV behaviors of the HL (3 mM) without and with CTDNA were studied with the scan rate of 100 mV/s and the results are shown in Fig. 4. It can be seen from Fig. 5, that in the absence of DNA (pure sample), the 1st voltammogram started in the positive direction, one oxidation peak was observed showing that HL is oxidizable in these conditions. No corresponding peak was observed in the reverse scan which indicated that the oxidation product of HL is

**Fig. 5.** Absorption spectra of 0.04 mM HL in the absence (a) and presence of 0.13 μM (b), 0.26 μM (c), 0.39 μM (d), 0.52 μM DNA (e). The arrow direction indicates increasing concentrations of DNA. Inset graph is the plot of $A_0/(A - A_0)$ vs. $1/[DNA]$ for the determination of binding constant and Gibbs free energy of HL-DNA Adduct at $\lambda_1 = 267$ nm and $\lambda_2 = 288$ nm.

not reducible. The attribution is strengthened by the appearance of irreversible anodic peak in the same CV region of guanine due to the oxidation of $-N=CH-$ group as reported by the earlier electrochemists [31,32]. The formal potential ($E^{o'}$) was found to be 0.596 V. In the presence of DNA (60 μ M and 120 μ M) the voltammetric peak currents decreased apparently, suggesting that there exists an interaction between the HL and CTDNA [33,34]. Bard has reported three kinds of modes for small molecules binding to DNA [35], if $E_{1/2}$ shifted to more negative value when small molecules interacted with DNA; the interaction mode was electrostatic binding. On the other hand, if $E_{1/2}$ shifted to more positive value, the interaction mode was intercalative binding. Therefore, it could be concluded that the HL could bind to DNA by intercalation because $E_{1/2}$ has shifted to positive value as shown in Fig. 4. In addition, considering the structure of the HL which has aromatic rings, we may deduce that it may bond to CTDNA more dominantly via an intercalation mode.

3.6. Conductometry

The conductance of HL in 80% ethanol at 25 °C falls in the range of 16 S cm² mol⁻¹, suggest its non electrolytic nature [32].

3.7. Absorption spectral features of CTDNA binding

The drug–DNA interaction can be carried out by UV–Visible absorption spectroscopy by monitoring the changes in the absorption properties of the drug or the DNA molecules. Drug–DNA interactions can be studied by comparison of UV–Visible absorption spectra of the free drug and drug–DNA complexes, which are usually different. Drug binding with DNA through intercalation usually results in hypochromism and bathochromism. Because of the intercalative mode involving a stacking interaction between an aromatic chromophore and the base pair of DNA, the extent of the hypochromism commonly parallels the intercalative binding strength [36,37].

The absorption spectrum of HL in the absence (a) and presence (b–e) of DNA is shown in Fig. 5. There exist two bands, one at 267 nm and other at 288 nm for free HL, respectively. With the addition of increasing concentration of DNA, the transition band at 267 exhibit hypochromism of 6.3%, 13%, 20.3%, 32.8% and 41% as well as hypsochromic shift (blue shift) of \sim 3.5 nm while at 288 nm exhibit hypochromism of 2.1%, 3.7%, 4.4%, 6.7% and 11.6% as well as bathochromic shift (red shift) of \sim 7 nm, respectively. These spectral characteristics suggest that the HL might bind to DNA by an intercalative mode as well as by groove binding. After intercalating the base pairs of DNA, the π^* orbital of the intercalated ligand could couple with π orbital of base pairs, thus decreasing the π – π^* transition energy, and further resulting in the bathochromism. On the other hand, the coupling of a π orbital with partially filled electrons decreases the transition probabilities hence results hypochromic shift. Since hypochromism due to π – π^* stacking interactions may appear in the case of the intercalative binding mode, while bathochromism (red-shift) may be observed when the DNA duplex is stabilized [38]. After 24 h, the spectrum was again taken and obtained the same results which conforms the stability of drug–DNA complex. Based upon the variation in absorbance, the intrinsic binding constant of the compound with DNA were determined according to Benesi–Hildebrand equation [36]:

$$\frac{A_0}{A - A_0} = \frac{\varepsilon_G}{\varepsilon_{H-G} - \varepsilon_G} + \frac{\varepsilon_G}{\varepsilon_{H-G} - \varepsilon_G} \times \frac{1}{K[\text{DNA}]}$$

where K is the association/binding constant, A_0 and A are the absorbances of the drug and its complex with DNA, respectively, and ε_G and ε_{H-G} are the absorption coefficients of the drug and

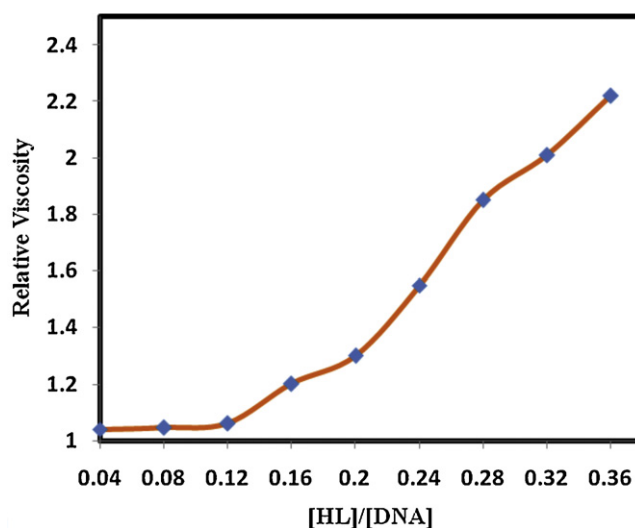


Fig. 6. Effects of increasing amount of HL on relative viscosity of CT-DNA at 25 \pm 0.1 °C. [DNA] = 2.37 \times 10⁻⁵ M.

the drug–DNA complex, respectively. The association constants were obtained from the intercept-to-slope ratios of $A_0/(A - A_0)$ vs. $1/[\text{DNA}]$ plots. The Gibb's free energy (ΔG) was determined from the equation:

$$\Delta G = -RT \ln K$$

where R is general gas constant (8.314 J K⁻¹ mol⁻¹) and T is the temperature (298 K).

Binding constants and Gibb's free energies were calculated for $\lambda_1 = 267$ nm and $\lambda_2 = 288$ nm. The binding constants were found to be 5.9 \times 10⁵ M⁻¹ and 1.1 \times 10⁶ M⁻¹ for λ_1 and λ_2 , respectively, while the Gibb's free energies were -14.3 kJ mol⁻¹ and -14.97 kJ mol⁻¹, respectively. Also it shows to some extent interaction with the minor grooves (λ_2) which may be due the hydrogen bonding to bases, typically to N3 of adenine and O2 of thymine [39] that results in bathochromism. The interaction of the drug with DNA is a spontaneous process as shown by the negative values of ΔG .

3.8. Viscosity measurements

To further clarify the binding modes of the HL with DNA, viscosity measurements were carried out. Hydrodynamic measurements that are sensitive to length change (i.e., viscosity) are regarded as the least ambiguous and the most critical tests of the binding model in solution. A classical intercalation model resulted in the lengthening of the DNA helix as the base pairs were separated to accommodate the binding complex, leading to an increase in DNA viscosity. In contrast, a partial, non-classical intercalation could bend (or kink) the DNA helix and reduce its effective length and, concomitantly, its viscosity. There is a marked effect of HL on the viscosity of CT-DNA as shown in Fig. 6. With an increasing amount of HL, the relative viscosity of DNA increases while the increasing amount of HL further increases the effective length of DNA which supports that HL bind through intercalation mode but with different affinity, i.e., also show some affinity for binding with grooves of DNA through hydrogen bonding. However, strong binding is presumably due to intercalation with DNA [40]. As shown in Fig. 6, the viscosity increases with the addition of the increasing amount of HL, therefore, intercalative mode, as a dominant mode, has selected for the interaction of HL with DNA. Since the viscosity first remains almost constant and then increases with increasing concentration

Table 4
Antibacterial activity of HL.

Compound	Average zone of inhibition (mm)					
	<i>Staphylococcus aureus</i>	<i>Klebsiella pneumoniae</i>	<i>Micrococcus luteus</i>	<i>Pseudomonas aeruginosa</i>	<i>Bordetella bronchiseptica</i>	<i>Escherichia coli</i>
HL	20	23	20	14.2	20	16
Roxythromycin	36	26	35	20	35	26
Cefixime	22	21	30	16	30	22
MIC ($\mu\text{g/mL}$)	500	250	1.95	62.5	500	250

Concentration: 1 mg/mL of DMSO. Reference drugs, Roxithromycin and Cefixime 1 mg/mL.

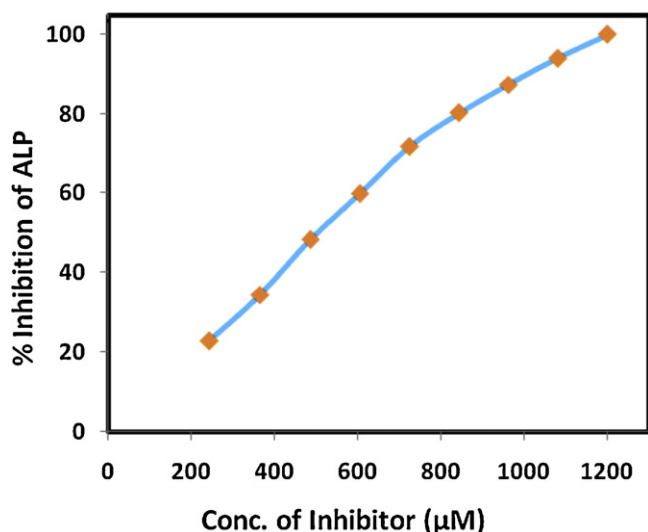


Fig. 7. % inhibition of the ALP enzyme vs. concentration of the HL (μM).

of HL, which indicates that groove binding also contribute to some extent.

3.9. Enzymatic study

The remarkable activity of the ligand may be due to OH group, which can play an important role in the enzymatic activity [41] and the imine group may impart in the elucidation of the mechanism of transformation reaction in biological system [42]. The results are shown in Fig. 7.

3.10. Antimicrobial activity and cytotoxicity

In vitro biological screening tests of the synthesized compound (HL) were carried out for antibacterial, antifungal, cytotoxicity. The antibacterial activity was tested against six bacterial strains: two Gram-positive [*M. luteus* (ATCC10240) and *S. aureus* (ATCC6538)] and four Gram-negative [*E. coli* (ATCC15224), *P. aeruginosa* (CM0559), *B. bronchiseptica* (ATCC4617) and *K. pneumoniae* (MTCC618)]. The agar well-diffusion method was used in these assays and each experiment was performed in triplicate. Readings of the zone of inhibition represents the mean value of three readings with standard deviation (SD), which are shown in

Table 5
Antifungal activity of HL.

Compound	Mean value of percent growth inhibition \pm SD				
	<i>Aspergillus flavus</i>	<i>Fusarium solani</i>	<i>Aspergillus niger</i>	<i>Mucor species</i>	<i>Aspergillus fumigates</i>
HL	30 \pm 0.045	71 \pm 0.056	65 \pm 0.035	63 \pm 0.040	61 \pm 0.038
Terbinafine	100	100	100	100	100

In vitro agar tube dilution method, concentration: 200 $\mu\text{g/mL}$ of DMSO. % inhibition of fungal growth = $100 - \text{gt/gc} \times 100$. gt = linear growth in test (mm) and gc = linear growth in vehicle control (mm).

Table 4. Roxithromycin and Cefixime were used as standard drugs in these assays. Criteria for activity is based on inhibition zone (mm); inhibition zone more than 20 mm shows significant activity, for 18–20 mm inhibition activity is good, 15–17 mm is low, and below 11–14 mm is non-significant activity. The antibacterial studies demonstrated that HL has activity toward tested bacteria. The values obtained for activity of HL against *S. aureus* and *M. luteus*, *K. pneumoniae* and *B. bronchiseptica* falls in category of significant activity while against *Pseudomonas* and *E. coli* showed low to non significant activity. HL was also subjected to antifungal activity against five fungal strains [*F. moniliformis*, *A. niger*, *F. solani*, *Mucor species* and *A. fumigatus*] by using Agar tube dilution method. The results are shown in Table 5. Terbinafine was used as standard drug in this assay. Criteria for activity is based on percent growth inhibition; more than 70% growth inhibition shows significant activity, 60–70% inhibition activity is good, 50–60% inhibition activity is moderate and below 50% inhibition activity is non-significant. The investigation shows that HL has significant to moderate activity against four strains while non significant activity was shown only against *flavus* [25,26]. Since Gram-negative bacteria are considered a quantitative microbiological method testing beneficial and important drugs in both clinical and experimental tumor chemotherapy [43], therefore the synthesized compound can be used for such purposes. Its anticancer and antitumor activities are under experiments and soon we will report them.

The cytotoxicity was studied by the brine-shrimp bioassay lethality method [25,26]. The LD₅₀ data show HL is toxic with LD₅₀ value in the range of 1.7598 $\mu\text{g/mL}$ in comparison to reference drug, MS-222 (*Tricaine methanesulfonate*) with LD₅₀ value of 4.3 $\mu\text{g/mL}$. The data are given in Table 6.

3.11. DPPH scavenging activity

The model of the scavenging of the stable DPPH radical is extensively used to evaluate antioxidant activities in less time than other methods. The reducing abilities of the HL were determined by their interaction with the free stable radical 1,1-diphenyl-2-picryl-hydrazyl (DPPH) at different concentrations. Antioxidants can react with DPPH and produce 1,1-diphenyl-2-picryl-hydrazine [44]. Due to its odd electron DPPH gives a strong absorption band at 517 nm appearing a deep violet color [45]. As this electron becomes paired off in the presence of a free radical scavenger, the absorption disappears and the resulting decolorization is stoichiometric with respect to the number of electrons taken up. The change of absorbance produced in this reaction is reviewed to evaluate the

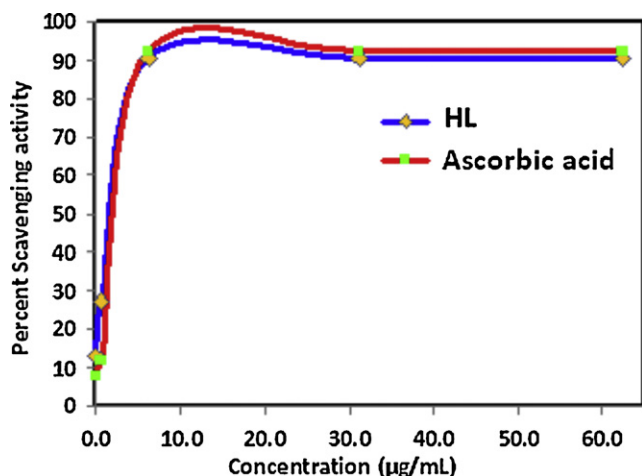


Fig. 8. Percent scavenging activity of DPPH vs. concentration ($\mu\text{g/mL}$) of HL.

Table 6
Cytotoxicity data of HL.

Compound	No. of shrimps killed out of 30 per dilution ^a			LD ₅₀ ^{b,c} ($\mu\text{g/mL}$)
	1000 $\mu\text{g/mL}$	100 $\mu\text{g/mL}$	10 $\mu\text{g/mL}$	
HL	30	25	23	1.7598
Vehicle control	0	0	0	

^a Against brine-shrimps (in vitro).

^b Data are based on mean value of 3 replicates each of 10, 100 and 1000 $\mu\text{g/mL}$.

^c Compared to standard drug MS-222 (*Tricaine methanesulfonate*) with LD₅₀ value of 4.30 $\mu\text{g/mL}$.

antioxidant potential of test samples and this assay is useful as a primary screening system [44]. The DPPH radical is a stable free radical (due to extensive delocalization of the unpaired electron) having λ_{max} at 517 nm. When this compound abstracts a hydrogen radical from HL then absorption vanishes due to the absence of free electron delocalization [46]. The percent scavenging activity of HL was calculated as:

$$\text{Scavenging activity (\%)} = \frac{A_0 - A_s}{A_0} \times 100$$

where A_s is the absorbance of the DPPH in the presence of the tested compound and A_0 is the absorbance of the DPPH in the absence of the tested compound (control) [9].

The effects of the HL have been shown in Fig. 8 with comparison to standard antioxidant ascorbic acid. The plots show that with increase in concentration of the test samples the intensity of radicals vanishes rapidly at a particular wavelength (517 nm). It has been observed that the HL showed maximum percentage of inhibition when it was incubated at a concentration of 62 $\mu\text{g/mL}$. The free ligand HL has scavenging activity between 7.8% and 90% within the investigated concentration range due to the OH group which can react with DPPH radical by the typical H-abstraction reaction (HAT) to form a stable macromolecular radical [47].

4. Supplementary material

Crystallographic data for the structure reported in this paper has been deposited with the Cambridge Crystallographic Data Centre, CCDC 836396 for HL. Copies of this information may be obtained free of charge from The Director, CCDC, 12, Union Road, Cambridge CB2 1EZ [Fax: +44 1223 336 033] or deposit@ccdc.cam.ac.uk or <http://www.ccdc.cam.ac.uk>.

Acknowledgment

The authors gratefully acknowledged Mr. Shafiq Ullah Marwat, Quaid-i-Azam University Islamabad, Pakistan, for his help in the cyclic voltammetry.

References

- [1] E. Hadjoudis, I.M. Mavridis, *Chem. Soc. Rev.* 33 (2004) 579–588.
- [2] A.A.A. Abu-Hussen, *J. Coord. Chem.* 59 (2006) 157–176.
- [3] M.S. Karthikeyan, D.J. Prasal, B. Poojary, K.S. Bhat, B.S. Holla, N.S. Kumari, *Bioorg. Med. Chem.* 14 (2006) 7482–7489.
- [4] K. Singh, M.S. Barwa, P. Tyagi, *Eur. J. Med. Chem.* 41 (2006) 147–153.
- [5] P. Panneerselvam, R.B. Nair, G. Vijayalakshmi, E.H. Subramanian, S.K. Sridhar, *Eur. J. Med. Chem.* 40 (2005) 225–229.
- [6] S.K. Sridhar, M. Saravanan, A. Ramesh, *Eur. J. Med. Chem.* 36 (2001) 615–625.
- [7] S.N. Pandeya, D. Sriram, G. Nath, E. DeClercq, *Eur. J. Pharm. Sci.* 9 (1999) 25–31.
- [8] R. Mladenova, M. Ignatova, N. Manolova, T. Petrova, I. Rashkov, *Eur. Polym. J.* 38 (2002) 989–999.
- [9] Z.A. Taha, A.M. Ajlouni, W. Al Momani, A.A. Al-Ghazawi, *Spectrochim. Acta A* 81 (2011) 570–577.
- [10] R. Atkins, G. Brewer, E. Kokot, G.M. Mockler, E. Sinn, *Inorg. Chem.* 24 (1985) 127–134.
- [11] S. Sobha, R. Mahalakshmi, N. Raman, *Spectrochim. Acta A* 92 (2012) 175–183.
- [12] A.K. Singh, V.K. Gupta, B. Gupta, *Anal. Chim. Acta* 585 (2007) 171–178.
- [13] N. Galic, Z. Cimerman, V. Tomisic, *Spectrochim. Acta A* 71 (2008) 1274–1280.
- [14] P.G. Cozzi, *Chem. Soc. Rev.* 33 (2004) 410–421.
- [15] A. Bolognese, G. Correale, M. Manfra, A. Lavecchia, O. Mazzoni, E. Novellino, V. Barone, A. Pani, E. Tramontano, P.L. Colla, C. Murgioni, I. Serra, G. Setzu, R. Lodo, *J. Med. Chem.* 45 (2002) 5205–5216.
- [16] Y.F. Xu, B.Y. Qu, X.H. Qian, Y.G. Li, *Bioorg. Med. Chem. Lett.* 15 (2005) 1139–1142.
- [17] X. Li, Y. Lin, Q. Wang, Y. Yuan, H. Zhang, X. Qian, *Eur. J. Med. Chem.* 46 (2011) 1274–1279.
- [18] W.L.F. Armarego, C.L.L. Chai, *Purification of Laboratory Chemicals*, 5th ed., Butterworth-Heinemann, London, New York, 2003.
- [19] S. Dey, S. Sarkar, H. Paul, E. Zangrando, P. Chattopadhyay, *Polyhedron* 29 (2010) 1583–1587.
- [20] C.V. Sastri, D. Eswaramoorthy, L. Giribabu, B.G. Maiya, *J. Inorg. Biochem.* 94 (2003) 138–145.
- [21] S. Mathur, S. Tabassum, *Cent. Eur. J. Chem.* 4 (3) (2006) 502–522.
- [22] J. Ahlers, *Biochem. J.* 149 (1975) 535–546.
- [23] K. Jiao, W. Sun, H.Y. Wang, *Chin. Chem. Lett.* 13 (1) (2002) 69–70.
- [24] K. Walter, C. Schutt, in: H.U. Bergmeyer (Ed.), *Methods of Enzymatic Analysis*, vol. 2, 2nd ed., Academic Press, Inc., New York, 1974, p. 860.
- [25] A. Rehman, M.I. Choudhary, W.J. Thomsen, *Bioassay Techniques for Drug Development*, Harwood Academic Publishers, Amsterdam, The Netherlands, 2001, p. 9.
- [26] B.N. Mayer, N.R. Ferrigni, J.E. Putnam, L.B. Jacobson, D.E. Nichols, J.L. McLaughlin, *Planta Med.* 45 (1982) 31–34.
- [27] A.F. Mutee, S.M. Salhimi, M.F. Yam, C.P. Lim, G.Z. Abdullah, O.Z. Ameer, M.F. Abdulkareem, M.Z. Asmawi, *Int. J. Pharmacol.* 6 (2010) 686–690.
- [28] G.K. Oloyede, M.J. Oke, Y. Raji, A.T. Olugbade, *World J. Chem.* 1 (5) (2010) 26–31.
- [29] A.P. Onocha, G.K. Oloyede, O.A. Bamkole, *Eur. J. Sci. Res.* 49 (3) (2011) 322–331.
- [30] Z. Popovic, V. Roje, G. Pavlovic, D. Matkovic-Calogovic, G. Giester, *J. Mol. Struct.* 597 (2001) 39–47.
- [31] A. Silvestri, G. Ruisi, R. Barbieri, *Hyperfine Interact.* 126 (2000) 43–46.
- [32] W. Rehman, M.K. Baloch, A. Badshah, *Eur. J. Med. Chem.* 43 (2008) 2380–2385.
- [33] Y.M. Song, P.J. Yang, M.L. Yang, J.W. Kang, S.Q. Qin, B.Q. Lv, *Trans. Met. Chem.* 28 (2003) 712–716.
- [34] Y.T. Li, W. Sun, Z.Y. Wu, Y.J. Zheng, C.W. Yan, *J. Inorg. Organomet. Polym.* 20 (2010) 586–591.
- [35] M.T. Carter, A.J. Bard, *J. Am. Chem. Soc.* 111 (1989) 8901–8911.
- [36] S. Shujha, A. Shah, Z. Rehman, N. Muhammad, S. Ali, R. Qureshi, N. Khalid, A. Meetsma, *Eur. J. Med. Chem.* 45 (2010) 2902–2911.
- [37] G.J. Chen, X. Qiao, P.Q. Qiao, G.J. Xu, J.Y. Xu, J.L. Tian, W. Gu, X. Liu, S.P. Yan, *J. Inorg. Biochem.* 105 (2011) 119–126.
- [38] G.Y. Bai, B. Dong, Y.Y. Lu, K.Z. Wang, L.P. Jin, L.H. Gao, *J. Inorg. Biochem.* 98 (2004) 2011–2015.
- [39] I. Haq, *Arch. Biochem. Biophys.* 403 (2002) 1–15.
- [40] J.L. Garcia-Gimenez, M. Gonzalez-Alvarez, M. Liu-Gonzalez, B. Macias, J. Borrás, G. Alzuet, *J. Inorg. Biochem.* 103 (2009) 923–934.
- [41] F.J. Huoa, C.X. Yin, Y.B. Wu, P. Yang, *Russ. J. Inorg. Chem.* 55 (7) (2010) 1087–1093.
- [42] A.S.A. Zidan, *Phosphorus Sulfur Silicon Relat. Elem.* 178 (2003) 567–582.
- [43] G.G. Mohamed, M.M. Omar, A.M.M. Hindy, *Spectrochim. Acta A* 62 (2005) 1140–1150.
- [44] D.N. Nicolaidis, D.R. Gautam, K.E. Litinas, D.J. Hadjipavlou-Litina, K.C. Fylaktakidou, *Eur. J. Med. Chem.* 39 (2004) 323–332.
- [45] T. Kulisic, A. Radonic, V. Katalinic, M. Milos, *Food Chem.* 85 (2004) 633–640.
- [46] C.A. Kontogiorgis, D. Hadjipavlou-Litina, *J. Enzyme Inhib. Med. Chem.* 18 (1) (2003) 63–69.
- [47] M.C. Foti, C. Daquino, C. Geraci, *J. Org. Chem.* 69 (2004) 2309–2314.